International Journal of Nanomedicine

Dovepress
open access to scientific and medical research

Open Access Full Text Article

ORIGINAL RESEARCH

pH and redox dual-responsive copolymer micelles with surface charge reversal for co-delivery of all-*trans*-retinoic acid and paclitaxel for cancer combination chemotherapy

This article was published in the following Dove Press journal:
International Journal of Nanomedicine

Yanqiu Zhang[1,2,*]
Lianjun Peng[3,*]
Jiahui Chu[4]
Ming Zhang[5]
Lizhu Sun[1,2]
Bin Zhong[5]
Qiyong Wu[5]

[1]Department of Oncology and Hematology, Shuyang Hospital Affiliated to Xuzhou Medical University, Suqian 223600, China; [2]Department of Oncology and Hematology, Shuyang People's Hospital, Suqian 223600, China; [3]Department of Respiratory, Central Hospital of Kaiping City, Kaiping 529300, China; [4]Department of Respiratory and Critical Care Medicine, Fuzong Clinical College of Fujian Medical University, Fuzhou General Hospital, Fuzhou, Fujian 350000, China; [5]Department of Thoracic and Cardiac Surgery, The Affiliated Changzhou No. 2 People's Hospital of Nanjing Medical University, Changzhou 213003, China

*These authors contributed equally to this work

Correspondence: Qiyong Wu; Bin Zhong
Department of Thoracic and Cardiac Surgery, The Affiliated Changzhou No. 2 People's Hospital of Nanjing Medical University, 29 Xinglong Xiang, Changzhou 213003, China
Tel +86 51988125373
Email wqyxycxy@aliyun.com; zsirr126@126.com; aprentis@sina.com

Background: Co-delivery all-trans-retinoic acid (ATRA) and paclitaxel (PTX) is an effective strategy for cancer therapy. However, in many previous reported ATRA conjugated co-delivery systems, the ATRA was released slower than PTX, and the total drug release of ATRA far lower than that of PTX.

Purpose: We designed and prepared a pH and redox dual responsive drug delivery system (DA-ss-NPs) co-delivery ATRA and PTX for cancer therapy. The surface charge of DA-ss-NPs could change from negative to positive under tumor slightly acidic microenvironment, and both drugs could be quickly released from DA-ss-NPs under intracellular high concentration of glutathione (GSH).

Methods: The DA-ss-NPs were constructed by encapsulating PTX into the hydrophobic core of the polymer micelles, in which the polymer was synthesized by conjugating ATRA and 2,3-Dimethylmalefic anhydride (DMA) on side chains of Cystamine dihydrochloride (Cys) modified PEG-*b*-PAsp (named DA-ss-NPs). The surface charge of DA-ss-NPs under different pH conditions were detected. And the drug release was also measured under different concentration of GSH. The therapeutic effect of DA-ss-NPs were investigated in Human lung cancer A549 cells and A549 tumor-bearing mice.

Results: The zeta potential of DA-ss-NPs was -16.3 mV at pH 7.4, and which changed to 16 mV at pH 6.5. Cell uptake experiment showed that more DA-ss-NPs were internalized by A549 cells at pH 6.5 than that at pH 7.4. In addition, in presence of 10 mM GSH at pH 7.4, about 75%-85% ATRA was released from DA-ss-NPs within 48 h; but less than 20% ATRA was released without GSH. In vivo antitumor efficiency showed that the DA-ss-NPs could affectively inhibite the tumor in compared with control groups.

Conclusion: The charge-reversal and GSH-responsive DA-ss-NPs provide an excellent platform for potential tumor therapy.

Keywords: all-*trans*-retionic acid, dual-responsive, charge reversal, PAsp, PEG-*b*-PLGA

Introduction

Cancer is one of the major causes of death around the world, and the treatment for cancer remains one of the principal challenges.[1] Chemotherapy is also one of the main strategies for cancer treatment in the clinic.[2] Combination chemotherapy, meaning simultaneous administration of two or multiple therapeutic agents, can cause synergetic responses, maximize the therapeutic effect, modulate different signaling pathways in cancer cells and overcome drug resistance and is widely used in the clinic.[3–5] For example, Vogus et al[6] developed a nanodrug delivery system based on the hyaluronic

submit your manuscript | www.dovepress.com
Dovepress
http://dx.doi.org/10.2147/IJN.S179046

acid for co-delivery of gemcitabine (GEM) and doxorubicin (DOX) to treat triple-negative breast cancer; the in vitro and in vivo experiments showed an effective synergistic therapeutic. Moreover, Zhao et al[7] reported a nano-in-nano polymer–dendrimer nanoparticle-based nanosystem to co-deliver paclitaxel (PTX) and DOX for combination cancer therapy.

All-*trans*-retinoic acid (ATRA), a metabolite of vitamin A, not only participates in various biological functions but also is a promising agent for cancer prevention and treatment.[8,9] However, it is reported that using ATRA alone in the clinical trial does not show a significant therapeutic effect in cancer patients.[10] However, when ATRA is combined with systemic chemotherapy, such as DOX and PTX, it resulted in good responses and significantly stabilized diseases in refractory metastatic breast cancer.[11] Moreover, because of the poor aqueous solubility, low plasma concentration and potential side effects, the clinical application of ATRA was limited.[12–14] To resolve this problem, many ATRA-conjugated nanoparticles for co-delivery of antitumor agents have been developed.[15–17] However, in these reports, the ATRA was covalently bonded to the polymers through the amine bond, which led to a slow drug release.[18–20] For example, Hou et al[13] developed a low molecular weight (MW) heparin-all-*trans*-retinoid acid conjugate nanocarrier for co-delivery of ATRA and PTX, in which <20% of ATRA was released within 20 days but about 70% of PTX was released.

Over the past decades, polyethylene glycol (PEG)-based polymers have been widely explored for drug delivery because the highly biocompatible macromolecule will prolong the blood circulation of micelles and prompt them to passively accumulate in the solid tumor tissues through the enhanced permeability and retention (EPR) effect.[21] However, the PEGylation appears to negatively affect the internalization of nanoparticles and can therefore be an obstacle to the realization of an effective therapeutic response.[22–24] It is reported that nanoparticles with cationic surface enter cells relatively easily because of adsorptive interaction with the cell membrane, while positively charged nanoparticles are easily cleared from blood circulation.[25–27] Therefore, if a nanoparticle could maintain its zeta potential as negative under blood circulation but switch to its zeta potential as positive at solid tumor environments, it could reduce the nonspecific protein adsorption and promote cellular uptake at the same time.[28,29]

It is well known that the extracellular pH of most tumor tissues is more acidic (pH 6.5–6.8) than that of normal tissues (pH 7.4), and the pH value of endosomes and lysosomes is about 4.5–6.5.[30–34] Thus, pH-responsive nanoparticles can be designed to control drug release at the specific tumor site. Moreover, the concentration of glutathione (GSH) in the cytoplasm (about 2–10 mM) is 100–1000-fold higher than that in the extracellular compartment.[23,35–37] In addition, GSH levels are found to be further increased in tumor tissues compared to those in the normal tissues.[35,38–40] Thus, disulfide linkage-based drug nanocarriers are able to promote drug release in the tumor cells.[41]

Keeping these issues in mind, a pH and redox dual-responsive drug delivery system with the surface charge-reversal drug delivery system for co-delivery of PTX and ATRA were designed to address difficulties in the drug delivery process (Scheme 1). First, cystamine dihydrochloride (Cys) was conjugated on the side of poly(ethylene glycol)-*block*-poly(β-benzyl-L-aspartate-*N*-carboxy-anhydride) (PEG-*b*-PBLA) through an ammonolysis reaction to obtain the redox-sensitive polymers (PEG-*b*-(PAsp-*g*-Cys)). Then, ATRA and 2,3-dimethylmalefic anhydride (DMA) were conjugated to the side of PEG-*b*-(PAsp-*g*-Cys) to produce the pH and redox stimuli-responsive polymer prodrug (PEG-*b*-(PAsp-*g*-ss-ATRA/DMA)). Finally, the polymer prodrug and PTX were assembled into drug-loaded micelle (DA-ss-NPs). The DA-ss-NPs micelle could keep negative charge under blood circulation but switch to positive charge under slightly acidic condition through the hydrolysis of DMA. Then, the disulfide-contained micelle was quickly uptaken by tumor cells and had rapid intracellular drug release because of the reductive conditions in tumor cells.[42] Therefore, the drug delivery system has great potential to achieve the goals including combined therapy, long circulation time, quick cellular uptake and rapid intracellular drug release.

Experimental

Materials

Amino-terminated methoxyl poly(ethylene glycol) (PEG-NH_2) was obtained from Sigma-Aldrich Co. (St Louis, MO, USA). The β-benzyl-L-aspartate was purchased from Sigma-Aldrich Co., and the β-benzyl-L-aspartate-*N*-carboxy-anhydride (BLA-NCA) was prepared by using the Fuchs-Farthing method.[43,44] PTX was purchased from Beijing Huafeng United Technology Company (Beijing, China). Cys, 1,6-hexanediamine (Hex), DMA, succinic anhydride (SA) and ATRA were all obtained from Aladdin Reagent Company (China, Shanghai, China).

Synthesis of PEG-*b*-PBLA

PEG-*b*-PBLA was synthesized according to literature.[42,45] Briefly, PEG-NH_2 (2.5 g, 0.5 mM) and BLA-NCA (3.95 g, 15 mM) were completely dissolved in anhydrous N,N-dimethylformamide (DMF). The reaction mixture was stirred for 48 hours at 40°C under a nitrogen atmosphere and then precipitated into excess cold diethyl ether to obtain the PEG-*b*-PBLA.

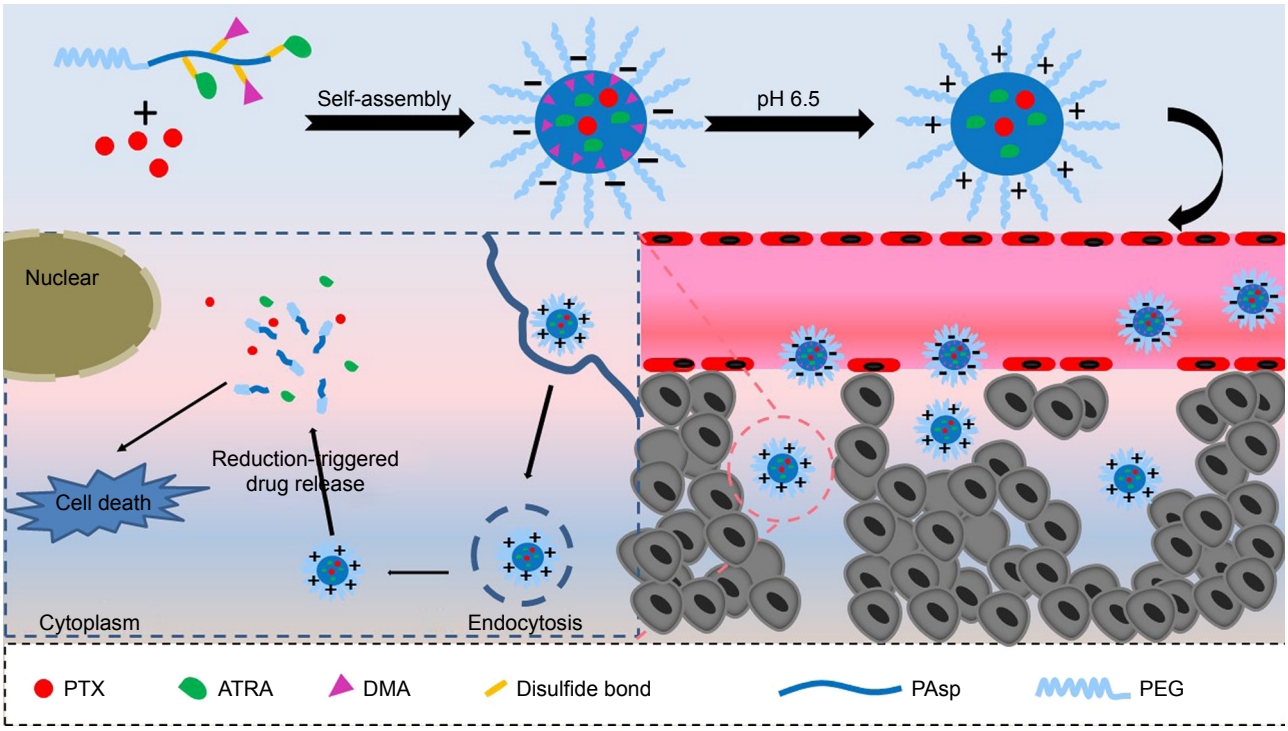

Scheme 1 Schematic illustration of pH and redox dual-responsive drug delivery system with the surface charge reversal for co-delivery of PTX and ATRA (their prolonged blood circulation, pH-triggered surface charge reversal and redox-responsive on-demand drug release and combined chemotherapy).
Abbreviations: PTX, paclitaxel; ATRA, all-*trans*-retinoic acid; DMA, 2,3-dimethylmalefic anhydride; PEG, polyethylene glycol.

Synthesis of PEG-*b*-(PAsp-*g*-Cys)

Poly(ethylene glycol)-*block*-poly([aspartic acid]-*graft*-[Cystamine dihydrochloride]) (PEG-*b*-(PAsp-*g*-Cys) was synthesized through ammonolysis reaction. In brief, Cys (2.4 g, 10 mM), PEG-b-PBLA (0.9 g, 0.1 mM) and triethylamine (3.25 mL) were dissolved in 40 mL dimethyl sulfoxide (DMSO) and stirred for 24 hours at room temperature under a nitrogen atmosphere. After that, the reaction mixture was dialyzed (MW: 3,500 Da) against methanol for 72 hours and distilled deionized water for 48 hours, and then, a white solid was obtained by lyophilization.[44]

As a control, no-redox-responsive polymers (PEG-*b*-(PAsp-*g*-Hex)) were also synthesized by using the same method; just Cys was changed to Hex.

Synthesis of PEG-*b*-(PAsp-*g*-ss-AR)

The ATRA was conjugated to the side chains of PEG-*b*-(PAsp-*g*-Cys) through the amidation reaction to obtain the PEG-*b*-(PAsp-*g*-ss-AR). Typically, ATRA (150 mg, 0.5 mM), 3 (ethyliminomethylideneamino)-N, N-dimethylpropan-1-amine, hydrochloride (96 mg, 0.5 mM) and n-hydroxysuccinimide (60 mg, 0.5 mM) were completely dissolved in 40 mL dry DMF and stirred for 2 hours at room temperature to activate the carboxyl of ATRA. Afterward, PEG-*b*-(PAsp-*g*-Cys) (900 mg, 0.1 mM) and 3.4 mL triethylamine (TEA) were dissolved in 30 mL dry DMF and then added dropwise to the above mixture reaction solution. The mixture solution was stirred for 24 hours at 40°C under a nitrogen atmosphere. The resulting solution was dialyzed against DMF for 72 hours and distilled water for 48 hours with a dialysis membrane (MW: 3,500 Da), followed by lyophilization to obtain ATRA conjugate: PEG-*b*-(PAsp-*g*-ss-AR). The amount of ATRA in PEG-*b*-(PAsp-*g*-ss-AR) was determined by ultraviolet (UV) absorption at 350 nm.[20]

As a control, ATRA was conjugated to the side chains of PEG-*b*-(PAsp-*g*-Hex) to obtain the no-redox-responsive polymer: PEG-*b*-(PAsp-*g*-cc-AR).

Synthesis of PEG-*b*-(PAsp-*g*-ss-AR/DMA)

PEG-*b*-(PAsp-*g*-ss-AR) (450 mg, 0.05 mM) and DMA (63 mg, 0.5 mM) were dissolved in DMF (15 mL), and then, TEA (200 μL) was added under nitrogen atmosphere. The mixture was stirred at room temperature for 24 hours. The resulting solution was dialyzed (MW: 3,500) against distilled water at pH 8–9 for 24 hours, followed by lyophilization to obtain the purpose polymer PEG-*b*-(PAsp-*g*-ss-AR/DMA).

On the other hand, DMA reacted with PEG-*b*-(PAsp-*g*-cc-AR) by using the same method to obtain the no-redox-responsive polymer with charge-reversal polymer: PEG-*b*-(PAsp-*g*-cc-AR/DMA).

Moreover, SA was grafted to PEG-*b*-(PAsp-*g*-ss-AR) by a similar procedure to obtain the non-charge-changing polymer: PEG-*b*-(PAsp-*g*-ss-AR/SA).

Preparation of drug-loaded micelle

To prepare the double drug-loaded micelles with redox-sensitive and charge-reversal polymer (named DA-ss-NPs), 20 mg PEG-*b*-(PAsp-*g*-ss-AR/DMA) and 6 mg PTX were dissolved in 3 mL of DMF and stirred at room temperature for 2 hours. After that, the mixture solution was added dropwise into 10 mL of PBS (0.01 M, pH 7.4) under vigorous stirring. The micelle solution was then dialyzed (MW: 3,500 Da) against PBS for 24 hours and filtered by a Millipore filter (pore size: 0.45 μm) to remove unencapsulated PTX. The drug loading content (DLC) and drug encapsulation efficiency (DEE) of PTX or ATRA were determined by HPLC or UV spectroscopy, respectively.

Additionally, the micelles formed from PEG-*b*-(PAsp-*g*-ss-AR) (positively charged nanoparticles, abbreviated as P-ss-NPs), PEG-*b*-(PAsp-*g*-cc-AR/DMA) (redox-insensitive nanoparticles, abbreviated as DA-cc-NPs) and PEG-*b*-(PAsp-*g*-ss-AR/SA) (non-charge-reversal nanoparticles, abbreviated as SA-ss-NPs) were prepared using the same method as that for DA-ss-NPs; just the PEG-*b*-(PAsp-*g*-ss-AR/DMA) was changed to the corresponding polymer. Furthermore, the coumarin-6-labeled micelles were also prepared, and the method was similar to that of DA-ss-NPs; just the PTX was changed to coumarin-6.

Characterization

The abovementioned facts about polymers were measured by nuclear magnetic resonance spectroscopy (^{1}H NMR) on a Bruker AVANCE III spectrometer at 300 MHz with DMSO-d_6 as the solvent. The size and the zeta potential of all micelles were determined using dynamic light scattering (DLS, ZS90; Malvern Instruments, Malvern, UK). The morphology of all micelles was investigated using transmission electron microscopy (TEM; Hitachi Ltd., Tokyo, Japan).

pH-induced zeta-potential change in the micelles

To study the surface charge characteristics of the micelles, DA-ss-NPs (0.1 mg/mL), P-ss-NPs and SA-ss-NPs (0.1 mg/mL) were dispersed in PBS (pH 6.5 or 7.4, 0.2 mM) and incubated at 37°C. Samples were taken at designated time intervals and the zeta potential was determined by DLS.

Disassembly and drug releasing of drug-loaded micelles

The disassembly of redox-sensitive DA-ss-NPs micelles in response to the various concentrations of GSH at different times was determined by DLS. In brief, 3 mL of DA-ss-NPs micelle solution containing GSH (0, 10 μM and 10 mM) was placed in an incubation shaker at 37°C and stirred at 100 rpm for 4 hours, and the changes in the sizes were measured by DLS. As a comparison, redox-no-sensitive DA-cc-NPs micelles incubated with and without 10 mM GSH were included as controls.

The drug released from DA-ss-NPs and DA-cc-NPs micelles at various concentrations of GSH was investigated using a dialysis method. Typically, 3 mL of DA-ss-NPs micelles containing 0.6 mg of PTX were enclosed in a clamped dialysis bag (MW: 3,500 Da) and immersed in 50 mL of PBS buffer solution (pH 7.4) containing 5% (w/v) Tween 80 and different concentrations of GSH (0, 10 μM and 10 mM). Every sample was gently shaken at an appropriate speed at 37°C. Then, at different time intervals, 1 mL of solute outside the dialysis bag was removed and replaced with equal volume of fresh medium. The amount of ATRA release was quantified using UV spectrophotometer at 350 nm. The quantification of PTX was performed on a HPLC system with a reversed-phase C18 column (250×4.6 mm, 5 μm) determined at 227 nm. The mobile phase consisted of acetonitrile/water 65:35 (v/v) at a flow rate of 1 mL/min.

Measure the stability of nanoparticles

The DA-ss-NPs, P-ss-NPs and SA-ss-NPs micelles were gently mixed with Roswell Park Memorial Institute (RPMI) 1640 culture medium with 10% FBS at pH 7.4 or 6.5. The size of these micelles after different periods of incubation time was determined by DLS.

Protein adsorption of the micelles

BSA and fibrinogen (FBG) were used as model proteins to study the protein adsorption of the micelles. The DA-ss-NPs, P-ss-NPs and SA-ss-NPs micelles were incubated with protein solutions in PBS at pH 6.5 or 7.4, with the final concentration of micelles and proteins fixed at 0.2 and 0.3 mg/mL. After incubation at 37°C for 2 hours, the aliquots of the samples were centrifuged at 10,000 rpm and the supernatants were collected to measure the BSA concentration using the commercial BCA Protein Assay Kit.[22] After that, the adsorbed proteins on the aggregate were calculated against a standard calibration curve of the BSA and FBG. The standards were analyzed at the same conditions.

Cells lines and animals

The human lung cancer cell line A549 was obtained from the Institute of Biochemistry and Cell Biology, Shanghai

Institutes for Biological Sciences, Chinese Academy of Sciences (Shanghai, China) and cultured in the RPMI 1640 culture medium, containing 10% (v/v) FBS and 100 IU/mL penicillin and 100 μg/mL streptomycin at 37°C in a humidified 5% CO_2 atmosphere.

BALB/c nude mice (male, 4–5 weeks, 20±2 g) were purchased from the Vital River Laboratory Animal Technology Co., Ltd. (Beijing, China). All animals received care in compliance with the guidelines outlined in the Guide for the Care and Use of Laboratory Animals, and all procedures were approved by the Shuyang Hospital Affiliated to Xuzhou Medical University Care and Use Committee.

In vitro cell uptake

A549 cells were seeded into six-well plates at a density of 1×10^5 cells/well and incubated for 24 hours under normal culture conditions. Then, the media were replaced with the RPMI 1640 medium containing the coumarin-6 labeled DA-ss-NPs, P-ss-NPs and SA-ss-NPs micelles at the concentration of 100 ng/mL of coumarin-6 at pH 7.4 or 6.5. Cells were incubated for 3 hours under normal culture conditions. After that, cells were washed twice with precooled PBS and fixed with 4% paraformaldehyde solution for 10 minutes, stained with Hoechst 33342 for 10 minutes, and then observed under an inverted fluorescence microscope (Leica Microsystems, Wetzlar, Germany).

HPLC analyses of cellular uptake of PTX with the different formation

A549 cells were seeded into six-well plates at a density of 3×10^4 cells per well in 2 mL of cell culture medium and incubated at 37°C for 24 hours. The original medium was replaced with DA-ss-NPs, DA-cc-NPs, P-ss-NPs and SA-ss-NPs in the RPMI 1640 medium of pH 6.5 or 7.4 and cultured for 1, 2 and 4 hours at 37°C, respectively. After incubation, the cells were washed three times with precooled PBS, added with 200 μL of cell lysis buffer (1% of Triton X-100) into each pore and incubated for 30 minutes at room temperature. After that, 100 μL of cell lysate was mixed with 200 μL of acetonitrile by ultrasonication for drug extraction followed by centrifugation at 8,000 rpm for 15 minutes; the supernatant was collected, and the concentration of PTX was detected by HPLC. All the determination of PTX concentration was normalized to the protein content of cell lysate.

In vitro cytotoxicity assay

First, the cytotoxicity of free drug combinations was studied by using the MTT assay. A549 cells were seeded into 96-well plates at a density of 5×10^3 cells per well and incubated overnight. Then, the cells were treated with free PTX, free ATRA and PTX+ATRA (mass ratio of PTX to ATRA was fixed at 1:1, 1:2 and 1:4, respectively) at different drug concentrations for 48 hours. The cell viability was analyzed using MTT and detected at 490 nm on a microplate reader (Thermo Multiskan MK3; Thermo Fisher Scientific, Waltham, MA, USA).[46,47] The combination index (CI) of two drugs was determined based on the additive effect of the two drugs effect equation according to the previous reports:[6,7]

$$CI = \frac{da}{Da} + \frac{dc}{Dc}$$

where *Da* and *Dc* denote the inhibitor concentration (IC) value of drug 1 alone and drug 2 alone, respectively. *da* and *dc* denote the concentration of drug 1 and drug 2 in the combination group at the IC value. CI>1 represents antagonism, CI=1 represents additive and CI<1 represents synergism.

The in vitro cytotoxicity of the drug-loaded micelles was evaluated against A549 cells by the MTT assay. The cells were seeded into a 96-well plate with a density of 5×10^3 cells per well and incubated overnight at 37°C in 5% CO_2 atmosphere. The culture medium was replaced with 200 μL of fresh medium without FBS containing DA-ss-NPs, DA-cc-NPs, P-ss-NPs or SA-ss-NPs at pH 7.4 or 6.5. After 4 hours incubation, the medium was removed and washed twice with PBS and 200 μL fresh medium at pH 7.4 was added. After another 45 hours incubation, the cell viability was analyzed using MTT and detected at 490 nm using a microplate reader (Thermo Multiskan MK3; Thermo Fisher Scientific).

In vivo tumor inhibition

Six-week-old male BALB/c nude mice were subcutaneously injected with 6×10^6 A549 cells at the right flank region. When the tumor size reached ~50–100 mm^3, the mice were randomly divided into seven groups (n=6) and intravenously injected with saline, free PTX, PTX+ATRA, DA-ss-NPs, DA-cc-NPs, P-ss-NPs or SA-ss-NPs every other day for four times. The dosages of PTX and ATRA were each 10 mg/kg. The tumor volume and mouse body weight were monitored every 2 days, and tumor size was calculated using the following formula: volume=0.5×(width)^2×(length). After treatment for 20 days, the mice were sacrificed and tumor section was harvested. Then, tumors were fixed in 4% (v/v) formalin saline for 1 day, followed by tissues embedded in paraffin and cut into a slice and then stained using H&E histopathological evaluation.

Statistical analysis

All the data were presented as mean±SD from at least three independent experiments. The differences among groups were calculated using Student's *t*-test or one-way ANOVA. Statistical analysis was performed using SPSS 20.0 software. Differences were considered as significant when $*P<0.05$, $**P<0.001$ and $***P<0.0001$.

Results and discussion

Synthesis and characterization of ATRA conjugates

The synthesized amphiphilic ATRA conjugates are shown in Scheme S1. First, PEG-*b*-PBLA was synthesized; then, Cys or Hex was conjugated to the side chain of PEG-*b*-PBLA through ammonolysis reaction; finally, ATRA, DMA or SA was conjugated to PEG-*b*-P(Asp-*g*-Cys) through ester or amide formation.

^{1}H NMR spectra of ATRA, PPEG-*b*-PBLG, PEG-*b*-(PAsp-*g*-Cys), PEG-*b*-(PAsp-*g*-ss-ATRA) and PEG-*b*-(PAsp-*g*-ss-ATRA/DMA) are shown in Figures S1–S3. All peaks in the spectra were well assigned according to references.[21,44,48] As determined by ^{1}H NMR spectroscopy of PEG-*b*-PBLA (Figure S1), there were 18 degrees of polymerization for PBLA blocks by comparing the integration of PEG with the integration of benzene of benzyloxycarbonyl.[48] According to the ^{1}H NMR spectra of PEG-*b*-PBLG and PEG-*b*-(PAsp-*g*-Cys), the disappearance of the peaks of the benzyl at 7.2 and 5.1 ppm demonstrated that the aminolysis reaction was successful (Figures S2 and S3). The characterization peaks of ATRA were at 1, 1.5–2.3 and 5.5–7.5 ppm; that of Cys was at 3.0 ppm and that of DMA was at 1–1.5 ppm.[29] These indicated successful conjugation of Cys, ATRA and DMA to PEG-*b*-PBLA.[21] The average amount of ATRA determined by UV–vis spectrophotometer was about 15.6%±1.22%.

Preparation and characterization of PTX-loaded micelles

To measure the optimal combination ratio of ATRA and PTX, the in vitro toxicity of A549 cells treated with free ATRA, free PTX and PTX+ATRA at various mass ratios was evaluated by MTT assay. The results showed that the minimum CI was achieved at a PTX/ATRA mass ratio of 1:1 (Figure S4); this result was same as previously reported.[49] Therefore, this mass ratio was selected as the optimal ratio for the following studies.

To determine the charge-reversal ability and redox-responsive drug release property, we prepared the DA-ss-NPs (charge reversal with redox-responsive micelle), SA-ss-NPs (non-charge switch and redox-sensitive micelle), P-ss-NPs (positive charge with redox-sensitive micelle) and DA-cc-NPs (charge reversal with redox-insensitive micelle) by mixing PTX and different ATRA-conjugated copolymers and simultaneously encapsulating into the hydrophobic core by a nano-co-precipitation method. The characterization data are shown in Table 1. The drug loading efficiency (DLC) of PTX and ATRA in DA-ss-NPs was 14.1%±3.5% and 13.7%±2.7%, respectively. There was no obvious difference in DLC of all micelles. All micelles form was determined by TEM; the images showed that all micelles were well dispersed with a regular spherical shape (Figure 1A–D), and their size was about 100 nm, which was consistent with the DLS detection results (Table 1).

pH-triggered surface charge reversal

To investigate micelles' surface charge-switchable property, different micelles were respectively dispersed in PBS at pH 6.5 or 7.4 and their charge was detected at predesigned time points. The results are shown in Figure 1E. All the micelles (excepted P-ss-NPs) revealed a nearly neutral constant surface charge at pH 7.4 during the incubation time, indicating that they were relatively stable at pH 7.4. While these micelles incubated at pH 6.5 for 4 hours, the surface charge of DA-ss-NPs was increased quickly and reached a positive zeta potential of about 16 mV within 1 hour, a little lower than P-ss-NPs, which might be not all the carboxyl groups dissociated and transformed to amino groups.[50] The charge of DA-cc-NPs also quickly changed to positive at short incubation time. In contrast, the zeta potential of SA-ss-NPs had barely changed during the incubation time. These results demonstrated that the DA-ss-NPs had a good charge transition ability.

Table 1 Characterization of PTX- and ATRA-loaded micelles

Micelles	Size (nm)	PDI	Zeta (mV)	DLC of PTX (%)	DEE of PTX (%)	DLC of ATRA (%)
DA-ss-NPs	122±12	0.22±0.02	−16.3±0.9	14.1±3.5	82±7.5	13.7±2.7
DA-cc-NPs	107±15	0.23±0.01	−17.2±0.9	13.6±3.7	79±6.2	13.7±1.9
SA-ss-NPs	119±18	0.29±0.03	−17±0.8	14.5±3.9	85±5.5	13.6±2.2
P-ss-NPs	132±22	0.33±0.02	27±1.7	12.9±2.7	74±9.1	13.8±2.1

Abbreviations: PTX, paclitaxel; ATRA, all-*trans*-retinoic acid; PDI, polydispersity index; DLC, drug loading content; DEE, drug encapsulation efficiency.

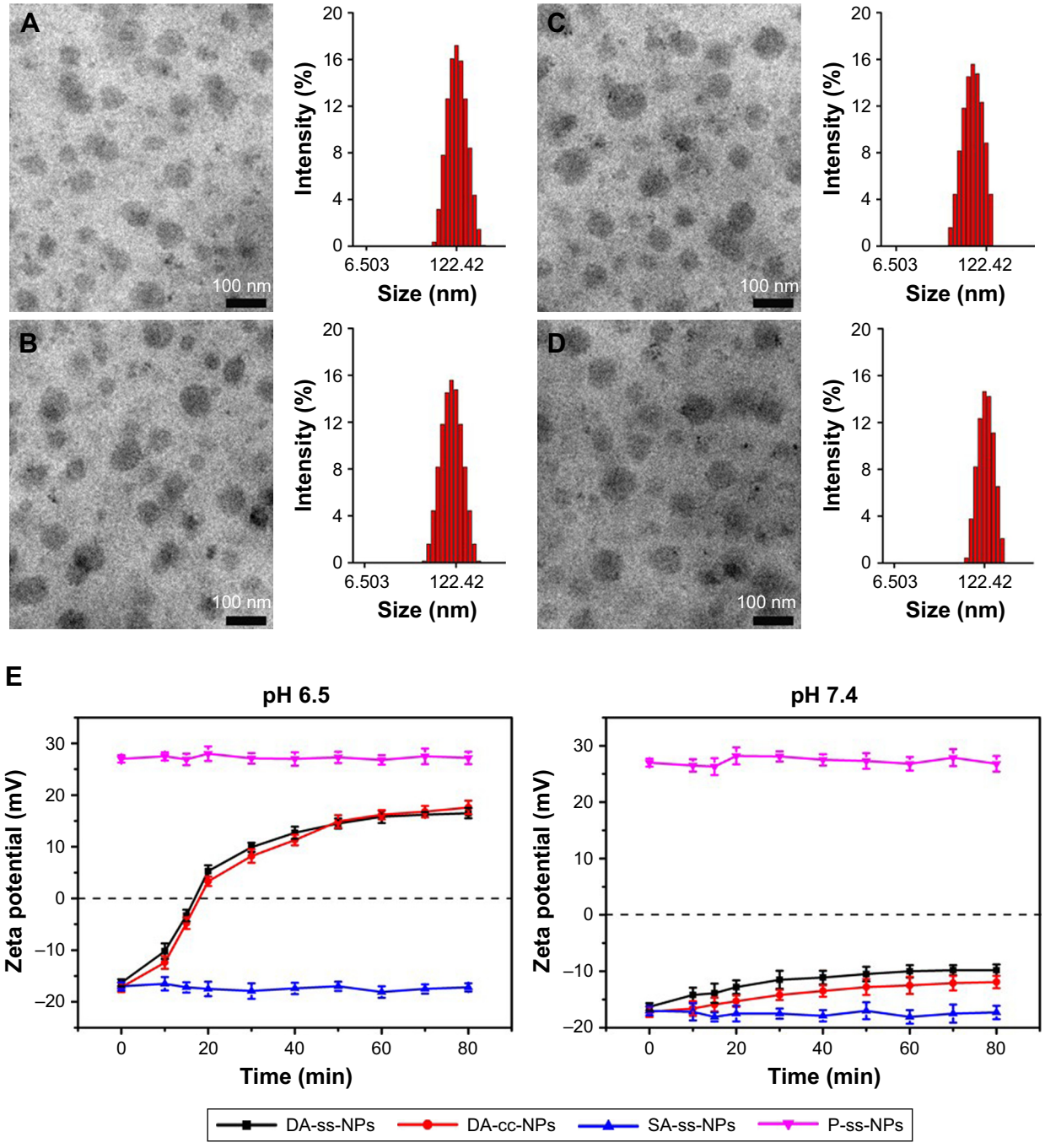

Figure 1 The TEM images and size of DA-ss-NPs (**A**), DA-cc-NPs (**B**), SA-ss-NPs (**C**) and P-ss-NPs (**D**). (**E**) Zeta-potential changes of DA-ss-NPs, DA-cc-NPs, SA-ss-NPs and P-ss-NPs as a function incubation time at pH 6.5 or pH 7.4 (mean±SD, n=3).
Abbreviation: TEM, transmission electron microscopy.

Protein adsorption experiment

Reduced nonspecific protein adsorption of the charged nanoparticles is an important indicator for the prolonged blood circulation.[51] Therefore, we have investigated the interaction of all micelles with proteins at different pH values by selecting BSA and FBG as models of plasma proteins.[52] As shown in Figure S5A, at neutral pH condition, both DA-ss-NPs and SA-ss-NPs exhibited slight protein adsorption (<15%) after 2 hours incubation, indicating that the negative potential on the surface of the micelles could contribute to prolonging their circulation time in blood. When the pH value decreased to 6.5, DA-ss-NPs strongly interacted with the proteins, showing that more than 80% protein adsorption occurred within 2 hours, nearly to the adsorption of P-ss-NPs (Figure S5B). However, SA-ss-NPs exhibited much less protein adsorption presented in the same conditions. The positive charge micelles P-ss-NPs showed stronger protein adsorption at all the measured pH values of 7.4 and 6.5. These results were in good agreement with

the pH-dependent charge conversion behavior of DA-ss-NPs at pH 6.5 and implied that micelles with a positive charge may potentially be cleared from blood circulation.[53]

Furthermore, to study the stability of the micelles, all of them were incubated in RPMI 1640 containing 10% FBS at pH 7.4 or 6.5. As shown in Figure S5C, at physiological pH condition, the sizes of DA-ss-NPs, DA-cc-NPs, and SA-ss-NPs exhibited little changes after incubated for 24 hours. While they were incubated at pH 6.5, the sizes of DA-ss-NPs and DA-cc-NPs quickly changed from about 100 nm to >600 nm within 2 hours, which might owe to the adsorption between micelles with proteins (Figure S5D). The SA-ss-NPs showed a negligible size change at the same conditions. Moreover, the size of the control P-ss-NPs showed a great change whether at pH 7.4 or pH 6.5. These results were consistent with the pH-dependent charge conversion behavior and protein adsorption of DA-ss-NPs at pH 6.5 and indicated that nanoparticles with positive charge might be unstable at blood circulation.

Redox-responsive micelles' disassembly and drug release

The time-dependent size change in DA-ss-NPs and DA-cc-NPs micelles under different conditions was investigated by DLS to present the redox-sensitive disassembly (Figure 2A and B). DA-ss-NPs and DA-cc-NPs micelles were quite stable at both pH 7.4 and 5.5 for 24 hours, indicating that these micelles could not disassemble at low pH. However, the average micelle

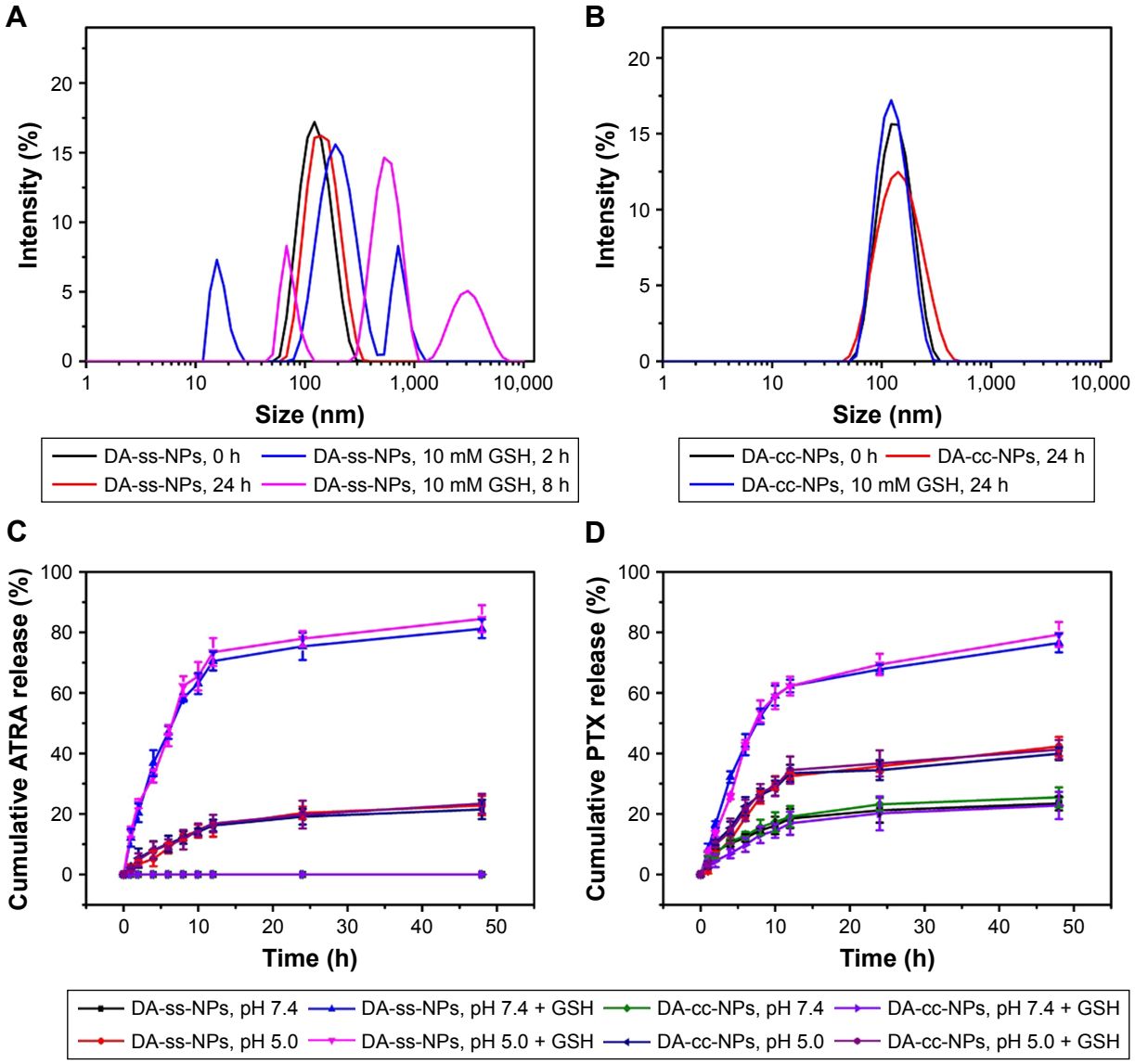

Figure 2 Size changes in DA-ss-NPs (**A**) and DA-cc-NPs (**B**) after incubating with or without GSH. Cumulative release of ATRA (**C**) and PTX (**D**) at pH 7.4 or 5.0 with or without GSH (mean±SD, n=3).
Abbreviations: GSH, glutathione; ATRA, all-*trans*-retinoic acid; PTX, paclitaxel.

size of DA-ss-NPs increased from 120 to about 358 nm, followed with additional 10 mM GSH, and the polydispersity index (PDI) changed from 0.21 to 0.53 within 2 hours; moreover, after incubation for 8 hours, the average particles size of DA-ss-NPs was changed from 120 to 695 nm and the PDI was changed from 0.21 to 0.73, which indicated the cleavage of the disulfide bond.[54] As a control, the size of DA-cc-NPs had no obvious change under different conditions.

It is well known that there exists a reductive condition in tumor cells. In our hypothesis, the PTX and ATRA would be quickly released from DA-ss-NPs under the reductive condition, but barely release in low pH value condition. In order to simulate the amide bond hydrolysis under acidic conditions to release ARTA, we prepared the DA-cc-NPs, and we hoped that ATRA and PTX would be slowly released from DA-cc-NPs under low pH environment. The drug release behavior is shown in Figure 2C and D. Little ATRA release was observed from DA-cc-NPs micelles within 48 hours in both the absence and the presence of 10 mM GSH. While under pH 5.5 with or without GSH conditions, about 15.3%±2.5% or 16.7%±3.7% ATRA was released from DA-cc-NPs within 48 hours, respectively, which might be contributed to the hydrolysis of amide bond under acidic environment. This phenomenon was also observed in DA-ss-NPs. However, when DA-ss-NPs incubated with GSH, a burst release of ATRA was observed, and about 75%–85% ARTA was released from DA-ss-NPs within 48 hours under pH 7.4 (normal physiological environment) or pH 5.5 (the pH in endosome of tumor cells). At pH 5.5, the release rate was slightly accelerated because of the higher hydrolysis of the amide bond under acidic condition.

PTX release profiles of DA-ss-NPs and DA-cc-NPs micelles are shown in Figure 2D. DA-ss-NPs and DA-cc-NPs micelles showed a slow release of PTX in the absence of GSH, and only 30% of the total PTX was released within 48 hours. In the presence of 10 mM GSH, no acceleration in PTX release was observed for DA-cc-NPs micelle, while PTX's release from DA-ss-NPs drastically accelerated, and about 70% of PTX was released from DA-ss-NPs within 48 hours. This might be due to the disassembly of DA-ss-NPs micelles induced by GSH.[38] These results suggested that DA-ss-NPs were triggered to release drug rapidly in response to highly redox environment after intracellular uptake.

Cell uptake of different micelles

In order to estimate whether the surface positive charge could enhance cellular internalization of nanoparticles, the cell uptake of DA-ss-NPs, DA-cc-NPs, P-ss-NPs and SA-ss-NPs in the human lung cancer cell A549 at pH 7.4 or 6.5 was qualitatively assessed by a fluorescence microscope. As shown in Figure 3A and B, after culturing with cells for 2 hours, the fluorescence intensity of P-ss-NPs was the strongest in A549 cells and there was no significant difference between pH 7.4 and 6.5. In contrast, no difference was observed when the cells were incubated with DA-ss-NPs, DA-cc-NPs and SA-ss-NP at pH 7.4. However, when the pH value was decreased to 6.5, the fluorescence intensity in A549 cells of DA-ss-NPs and DA-cc-NPs was obviously stronger than in those of SA-ss-NPs and nearly reached with those of P-ss-NPs. These results demonstrated that the response of DA-ss-NPs to the low pH value of the tumor microenvironment could enhance their uptake by the tumor cells.

To further demonstrate this phenomenon, we quantitatively evaluated the intracellular concentration of PTX after incubation for 1 hour, 2 hours and 4 hours at different pH values. As shown in Figure 3C and D, cell uptake of PTX with different forms was dose dependent, and the concentration of PTX within A549 cells incubated with DA-ss-NPs, DA-cc-NPs and SA-ss-NPs was very low. When cells incubated with P-ss-NPs at pH 7.4 or 6.5, the intracellular concentration of PTX had no significant difference and was the highest. In contrast, after incubating with DA-ss-NPs and DA-cc-NPs at pH 6.5, the intracellular concentration of PTX was significantly higher than that of cultured SA-ss-NP. These results are consistent with the previous quantitative results.

In vitro cytotoxicity assay

The aim of this study was to demonstrate that the charge-reversal micelles could promote cellular uptake and the quick release of ATRA could enhance the synergy therapy with PTX. To verify this assumption, we have evaluated the viability of the A549 cells after incubation with different micelles at different pH values by MTT. Many studies have shown that PTX and ATRA have synergistic anticancer effects;[18–20] thus, in the present study, we have not detected the cytotoxicity of free PTX, ATRA and PTX+ATRA. As shown in Figure 3E and F, all the micelles had a dose-dependent effect on the cell viability. The cell viabilities of A549 after treating with positive charge P-ss-NPs micelles were all $<$20% in the presence of pH 7.4 or 6.5 when the dose of PTX reached 50 μg/mL. At pH 7.4, the cell viabilities of A549 cells treated with DA-ss-NPs were about 70% even if the highest dose of PTX reached 50 μg/mL. In contrast, the cell viabilities of A549 cells incubated with DA-ss-NPs were $<$25% under pH 6.5, while the dose of PTX reached to 50 μg/mL. Compared to the charge-reversal DA-ss-NPs, the cell viabilities of A549 cells cultured with non-charge-reversal SA-ss-NPs were all $>$70% at pH 7.4 and pH 6.5 at all dose of the drug. These demonstrated that pH-sensitive,

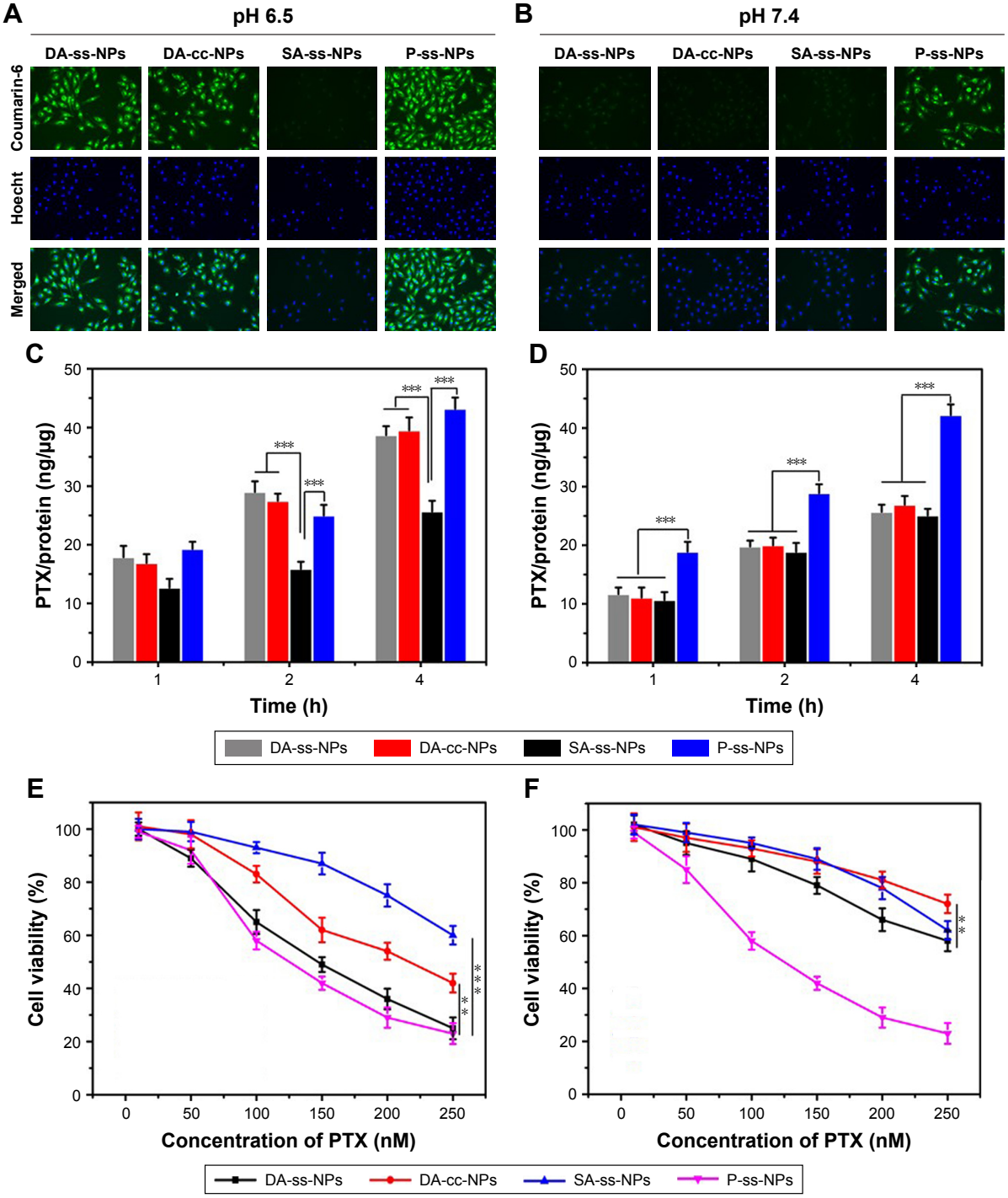

Figure 3 Fluorescence microscope images of A549 cells after incubating with DA-ss-NPs, DA-cc-NPs, SA-ss-NPs and P-ss-NPs for 2 hours at pH 6.5 (**A**) or pH 7.4 (**B**). Cellular accumulation of PTX at pH 6.5 (**C** and **D**) in A549 cells after incubating with DA-ss-NPs, DA-cc-NPs, SA-ss-NPs or P-ss-NPs. **E**–**F**: Cell viabilities of A549 cells after incubating with DA-ss-NPs, DA-cc-NPs, SA-ss-NPs or P-ss-NPs at pH 6.5 (**E**) and pH 7.4 (**F**) through MTT assay (mean±SD, n=6, $^{**}P<0.02$, $^{***}P<0.001$).
Abbreviation: PTX, paclitaxel.

charge-switchable DA-ss-NPs showed a more effective inhibition proliferation against cancer cells at tumor extracellular pH value than SA-ss-NPs. These results were similar to those of previous reports.[29,52]

Moreover, at pH 7.4, the cell viabilities of A549 cells after treating with DA-cc-NPs were higher than 75% at all concentration and higher than those of DA-ss-NPs at the same conditions. However, when the pH decreased to 6.5, the cell viabilities of A549 were also higher than 55% after incubating with DA-cc-NPs, which were significantly higher than the viabilities of cells treated with DA-ss-NPs at the same conditions. As mentioned earlier in this paper, cellular uptake of DA-ss-NPs and DA-cc-NPs had no obvious difference, but the drug release rate of DA-cc-NPs was slower than that of DA-ss-NPs at the

same conditions. Therefore, we could conclude that the cell inhibition proliferation against A549 cells of DA-ss-NPs was more effective than that of DA-cc-NPs, which contributed to the slow intracellular drug release, and the root cause was the slow hydrolysis of the amide bond at pH 5.0. This phenomenon was also similar to that of the previous report.[10] Therefore, these results have demonstrated that our hypothesis is true.

In vivo antitumor efficiency

To further explore the abovementioned results, the in vivo antitumor efficiency of all micelles was evaluated using human lung cancer A549 tumor-bearing nude mice. Tumor-bearing mice were randomly divided into seven groups with six mice in each group: PBS, PTX (free PTX), PTX+ATRA (free PTX and free ATRA), DA-ss-NPs, DA-cc-NPs and SA-ss-NPs. When the tumor grew to a size of about 50–100 mm^3, 1 week after inoculation of the cancer cells, different formulations with equivalent doses of PTX (10.0 mg/kg) and ATRA (2.5 mg/kg) were given via tail intravenous (i.v.) injection.[55]

The tumor size was measured every other day. As shown in Figure 4A, the growth of tumor was inhibited to a certain extent after the treatment with all drug formations compared with PBS control group. Administration of SA-ss-NPs and DA-cc-NPs resulted in a slightly better inhibition of tumor growth, while treating with DA-ss-NPs showed a more significant inhibition of tumor growth compared with treating with SA-ss-NPs or DA-cc-NPs. The slight tumor inhibition for DA-cc-NPs indicated that the slow drug release could not completely eliminate the tumor. The tumor weight and volume of the excised tumor (Figure 4B and D) agreed well with those measured in living mice (Figure 4A). Meanwhile, the body weight of mice remained stable during the treatment, suggesting no significant systemic toxicity for all formulations (Figure 4C). The histologic images of the tumor section stained by H&E showed the highest level of tumor cell nuclear ablation after treatment with DA-ss-NPs as shown in Figure 4E. These results demonstrated that the DA-ss-NPs had a good antitumor potential in vivo.

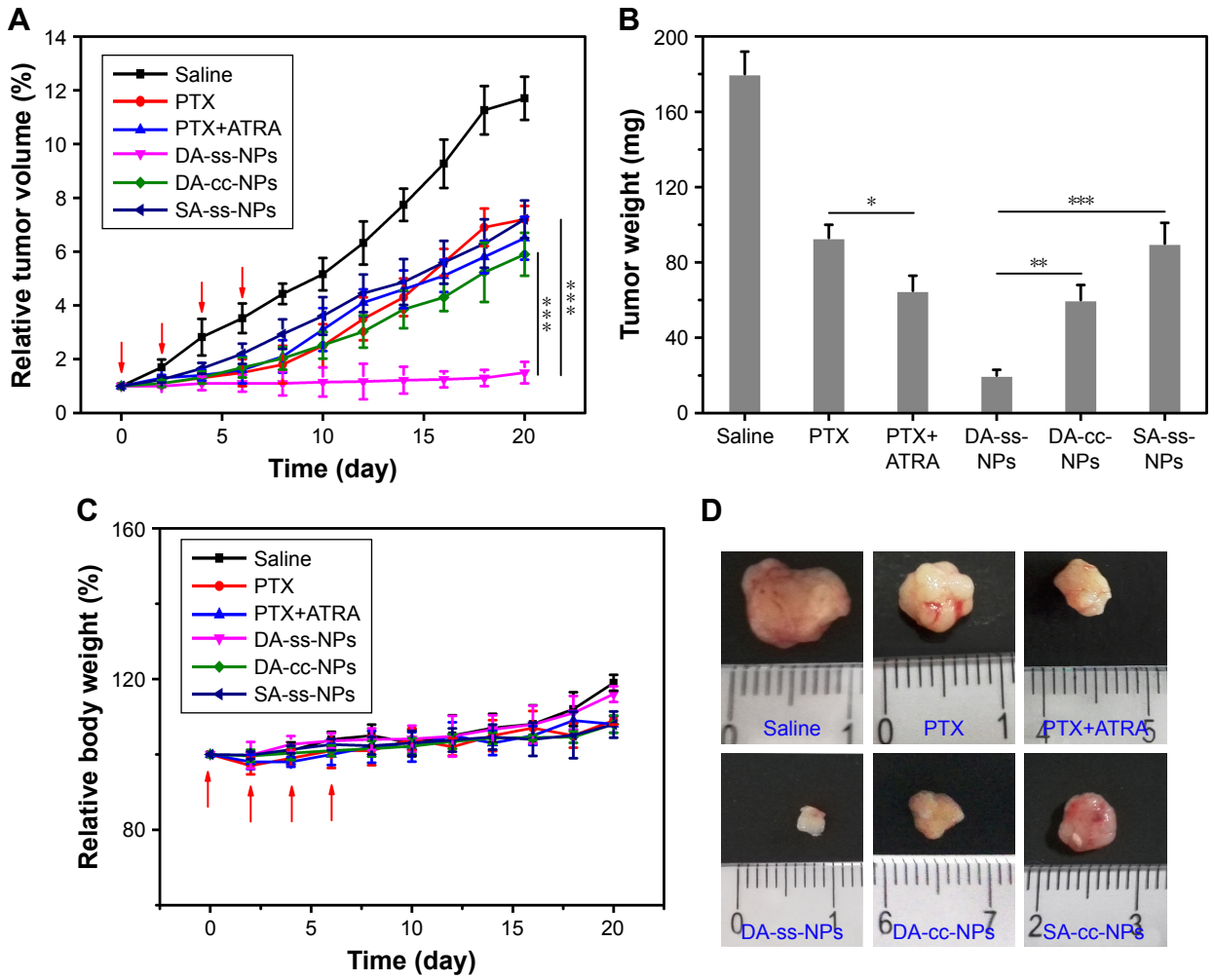

Figure 4 (*Continued*)

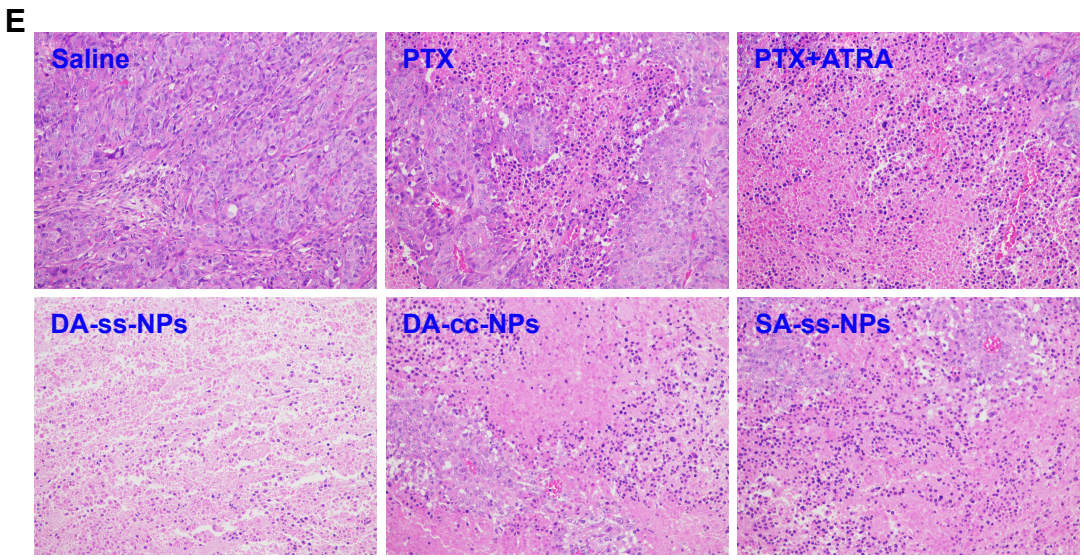

Figure 4 In vivo antitumor effect of all drug formations.
Notes: (**A**) Tumor volumes of different groups of tumor-bearing mice at different days after treating with physiological saline, free PTX, PTX+ATRA, DA-ss-NPs, DA-cc-NPs, SA-ss-NPs and P-ss-NPs (***significant difference between DA-ss-NPs and DA-cc-NPs or SA-ss-NPs). (**B**) Excised tumor weight of different groups. (**C**) Mice weight of different treatment groups. (**D**) Photos of excised tumors. (**E**) Histology analysis by H&E staining was performed for the different treatment groups using a virtual microscope (200× vision). All data were represented as mean±SD. n=6, *$P<0.05$, **$P<0.01$ and ***$P<0.001$.
Abbreviations: PTX, paclitaxel; ATRA, all-*trans*-retinoic acid.

Conclusion

We have developed a pH-triggered surface charge reversal with redox-responsive rapid drug release polymer micelle co-loaded with PTX and ATRA for combination anticancer therapy. The micelle thus exhibited prolonged circulation time owing to the reduced nonspecific protein absorption of the negative charge at natural condition, while the response of micelle to acidic condition resulted in switching to being positively charged and hence further promoting the cancer cell internalization in vivo and then rapidly releasing drug under a high concentration of GSH environment, which in turn resulted in an increased inhibition of tumor growth. The rapid release of two drugs at the same time significantly enhanced the antitumor efficiency in vivo. The described technology unifies the surface charge reversal, on-demand quick drug release, combination therapy and excellent biocompatibility into one formulation and hence has a great potential to achieve better therapeutic effects in cancer treatment.

Acknowledgment

This work was supported by the Changzhou City Science and Technology Project (CJ20159056).

Disclosure

The authors report no conflicts of interest in this work.

References

1. Hu Q, Sun W, Wang C, Gu Z. Recent advances of cocktail chemotherapy by combination drug delivery systems. *Adv Drug Deliv Rev*. 2016;98:19–34.
2. Depinho RA. The age of cancer. *Nature*. 2000;408(6809):248–254.
3. Hu CM, Zhang L. Nanoparticle-based combination therapy toward overcoming drug resistance in cancer. *Biochem Pharmacol*. 2012;83(8):1104–1111.
4. Bozic I, Reiter JG, Allen B, et al. Evolutionary dynamics of cancer in response to targeted combination therapy. *Elife*. 2013;2:e00747.
5. Bang Y-J, Van Cutsem E, Feyereislova A, et al. Trastuzumab in combination with chemotherapy versus chemotherapy alone for treatment of HER2-positive advanced gastric or gastro-oesophageal junction cancer (ToGA): a phase 3, open-label, randomised controlled trial. *The Lancet*. 2010;376:687–697.
6. Vogus DR, Evans MA, Pusuluri A, et al. A hyaluronic acid conjugate engineered to synergistically and sequentially deliver gemcitabine and doxorubicin to treat triple negative breast cancer. *J Control Release*. 2017;267:191–202.
7. Zhao Z, Lou S, Hu Y, Zhu J, Zhang C. A Nano-in-Nano Polymer-Dendrimer Nanoparticle-Based Nanosystem for Controlled Multidrug Delivery. *Mol Pharm*. 2017;14(8):2697–2710.
8. Bushue N, Wan YJ, Y-Jy W. Retinoid pathway and cancer therapeutics. *Adv Drug Deliv Rev*. 2010;62(13):1285–1298.
9. Okuno M, Kojima S, Matsushima-Nishiwaki R, et al. Retinoids in cancer chemoprevention. *Curr Cancer Drug Targets*. 2004;4(3):285–298.
10. Sutton LM, Warmuth MA, Petros WP, Winer EP. Pharmacokinetics and clinical impact of all-trans retinoic acid in metastatic breast cancer: a phase II trial. *Cancer Chemother Pharmacol*. 1997;40(4):335–341.
11. Bryan M, Pulte ED, Toomey KC, et al. A pilot phase II trial of all-trans retinoic acid (Vesanoid) and paclitaxel (Taxol) in patients with recurrent or metastatic breast cancer. *Invest New Drugs*. 2011;29(6):1482–1487.
12. Zuccari G, Bergamante V, Carosio R, et al. Micellar complexes of all-trans retinoic acid with polyvinylalcohol-nicotinoyl esters as new parenteral formulations in neuroblastoma. *Drug Deliv*. 2009;16(4):189–195.
13. Hou L, Fan Y, Yao J, et al. Low molecular weight heparin-all-trans-retinoid acid conjugate as a drug carrier for combination cancer chemotherapy of paclitaxel and all-trans-retinoid acid. *Carbohydr Polym*. 2011;86(3):1157–1166.
14. Chung KD, Jeong YI, Chung CW, Kim DH, Kang DH. Anti-tumor activity of all-trans retinoic acid-incorporated glycol chitosan nanoparticles against HuCC-T1 human cholangiocarcinoma cells. *Int J Pharm*. 2012;422(1–2):454–461.

15. Sun R, Liu Y, Li SY, et al. Co-delivery of all-trans-retinoic acid and doxorubicin for cancer therapy with synergistic inhibition of cancer stem cells. *Biomaterials*. 2015;37:405–414.
16. Ni J, Tian F, Dahmani FZ, et al. Curcumin-carboxymethyl chitosan (CNC) conjugate and CNC/LHR mixed polymeric micelles as new approaches to improve the oral absorption of P-gp substrate drugs. *Drug Deliv*. 2016;23(9):3424–3435.
17. Castleberry SA, Quadir MA, Sharkh MA, Shopsowitz KE, Hammond PT. Polymer conjugated retinoids for controlled transdermal delivery. *J Control Release*. 2017;262:1–9.
18. Zhang J, Han J, Zhang X, et al. Polymeric nanoparticles based on chitooligosaccharide as drug carriers for co-delivery of all-trans-retinoic acid and paclitaxel. *Carbohydr Polym*. 2015;129:25–34.
19. Yao J, Zhang L, Zhou J, Liu H, Zhang Q. Efficient simultaneous tumor targeting delivery of all-trans retinoid acid and Paclitaxel based on hyaluronic acid-based multifunctional nanocarrier. *Mol Pharm*. 2013;10(3):1080–1091.
20. Li J, Jiang X, Guo Y, et al. Linear-dendritic copolymer composed of polyethylene glycol and all-trans-retinoic acid as drug delivery platform for paclitaxel against breast cancer. *Bioconjug Chem*. 2015;26(3):418–426.
21. Oh NM, Kwag DS, Oh KT, et al. Electrostatic charge conversion processes in engineered tumor-identifying polypeptides for targeted chemotherapy. *Biomaterials*. 2012;33(6):1884–1893.
22. Huo Q, Zhu J, Niu Y, et al. pH-triggered surface charge-switchable polymer micelles for the co-delivery of paclitaxel/disulfiram and overcoming multidrug resistance in cancer. *Int J Nanomedicine*. 2017;12:8631–8647.
23. Fang Y, Xue J, Gao S, et al. Cleavable PEGylation: a strategy for overcoming the "PEG dilemma" in efficient drug delivery. *Drug Deliv*. 2017;24(Supp 1):22–32.
24. Jin M, Jin G, Kang L, et al. Smart polymeric nanoparticles with pH-responsive and PEG-detachable properties for co-delivering paclitaxel and survivin siRNA to enhance antitumor outcomes. *Int J Nanomedicine*. 2018;13:2405–2426.
25. Fang J, Nakamura H, Maeda H. The EPR effect: Unique features of tumor blood vessels for drug delivery, factors involved, and limitations and augmentation of the effect. *Adv Drug Deliv Rev*. 2011;63(3):136–151.
26. Cho EC, Xie J, Wurm PA, Xia Y. Understanding the role of surface charges in cellular adsorption versus internalization by selectively removing gold nanoparticles on the cell surface with a I2/KI etchant. *Nano Lett*. 2009;9(3):1080–1084.
27. Feng S, Zhang H, Zhi C, Gao XD, Nakanishi H. pH-responsive charge-reversal polymer-functionalized boron nitride nanospheres for intracellular doxorubicin delivery. *Int J Nanomedicine*. 2018;13:641–652.
28. du JZ, Sun TM, Song WJ, Wu J, Wang J. A tumor-acidity-activated charge-conversional nanogel as an intelligent vehicle for promoted tumoral-cell uptake and drug delivery. *Angew Chem Int Ed Engl*. 2010;49(21):3621–3626.
29. Wang Y, Lv S, Deng M, et al. A charge-conversional intracellular-activated polymeric prodrug for tumor therapy. *Polym Chem*. 2016;7(12):2253–2263.
30. Zhu J, Niu Y, Li Y, et al. Stimuli-responsive delivery vehicles based on mesoporous silica nanoparticles: recent advances and challenges. *J Mater Chem B*. 2017;5(7):1339–1352.
31. Chen WL, Li F, Tang Y, et al. Stepwise pH-responsive nanoparticles for enhanced cellular uptake and on-demand intracellular release of doxorubicin. *Int J Nanomedicine*. 2017;12:4241–4256.
32. Fan B, Xing Y, Zheng Y, et al. pH-responsive thiolated chitosan nanoparticles for oral low-molecular weight heparin delivery: *in vitro* and *in vivo* evaluation. *Drug Deliv*. 2016;23(1):238–247.
33. Zhou Q, Zhang L, Yang T, Wu H. Stimuli-responsive polymeric micelles for drug delivery and cancer therapy. *Int J Nanomedicine*. 2018;13:2921–2942.
34. Shen Y, Zhang J, Hao W, et al. Copolymer micelles function as pH-responsive nanocarriers to enhance the cytotoxicity of a HER2 aptamer in HER2-positive breast cancer cells. *Int J Nanomedicine*. 2018;13:537–553.
35. Taghizadeh B, Taranejoo S, Monemian SA, et al. Classification of stimuli-responsive polymers as anticancer drug delivery systems. *Drug Deliv*. 2015;22(2):145–155.
36. Zhang J, Fang X, Li Z, et al. Redox-sensitive micelles composed of disulfide-linked Pluronic-linoleic acid for enhanced anticancer efficiency of brusatol. *Int J Nanomedicine*. 2018;13:939–956.
37. Lin J, Zhao C, Liu C, et al. Redox-responsive F127-folate/F127-disulfide bond-d-α-tocopheryl polyethylene glycol 1000 succinate/P123 mixed micelles loaded with paclitaxel for the reversal of multidrug resistance in tumors. *Int J Nanomedicine*. 2018;13:805–830.
38. Sun J, Liu Y, Chen Y, et al. Doxorubicin delivered by a redox-responsive dasatinib-containing polymeric prodrug carrier for combination therapy. *J Control Release*. 2017;258:43–55.
39. Tan S, Wang G. Redox-responsive and pH-sensitive nanoparticles enhanced stability and anticancer ability of erlotinib to treat lung cancer in vivo. *Drug Des Devel Ther*. 2017;11:3519–3529.
40. Li J, Xu R, Lu X, He J, Jin S. A simple reduction-sensitive micelles co-delivery of paclitaxel and dasatinib to overcome tumor multidrug resistance. *Int J Nanomedicine*. 2017;12:8043–8056.
41. Song Q, Chuan X, Chen B. A smart tumor targeting peptide-drug conjugate, pHLIP-SS-DOX: synthesis and cellular uptake on MCF-7 and MCF-7/Adr cells. *Drug Deliv*. 1734;2015:23.
42. Park CW, Yang H-M, Woo M-A, et al. Completely disintegrable redox-responsive poly(amino acid) nanogels for intracellular drug delivery. *Journal of Industrial and Engineering Chemistry*. 2017;45:182–188.
43. Alani AW, Bae Y, Rao DA, Kwon GS. Polymeric micelles for the pH-dependent controlled, continuous low dose release of paclitaxel. *Biomaterials*. 2010;31(7):1765–1772.
44. Jiang Y, Wang X, Liu X, et al. Enhanced Antiglioma Efficacy of Ultrahigh Loading Capacity Paclitaxel Prodrug Conjugate Self-Assembled Targeted Nanoparticles. *ACS Appl Mater Interfaces*. 2017;9(1):211–217.
45. Wang F, Wang YC, Dou S, Xiong MH, Sun TM, Wang J. Doxorubicin-tethered responsive gold nanoparticles facilitate intracellular drug delivery for overcoming multidrug resistance in cancer cells. *ACS Nano*. 2011;5(5):3679–3692.
46. You Y, Xu Z, Chen Y. Doxorubicin conjugated with a trastuzumab epitope and an MMP-2 sensitive peptide linker for the treatment of HER2-positive breast cancer. *Drug Deliv*. 2018;25(1):448–460.
47. Yin X, Feng S, Chi Y, et al. Estrogen-functionalized liposomes grafted with glutathione-responsive sheddable chotooligosaccharides for the therapy of osteosarcoma. *Drug Deliv*. 2018;25(1):900–908.
48. Zhang Y, Li P, Pan H, et al. Retinal-conjugated pH-sensitive micelles induce tumor senescence for boosting breast cancer chemotherapy. *Biomaterials*. 2016;83:219–232.
49. Hong GY, Jeong YI, Lee SJ, Lee E, Oh JS, Lee HC. Combination of paclitaxel- and retinoic acid-incorporated nanoparticles for the treatment of CT-26 colon carcinoma. *Arch Pharm Res*. 2011;34(3):407–417.
50. Du JZ, Du XJ, Mao CQ, Wang J. Tailor-made dual pH-sensitive polymer-doxorubicin nanoparticles for efficient anticancer drug delivery. *J Am Chem Soc*. 2011;133(44):17560–17563.
51. Wu L, Wu M, Lin X, et al. Magnetite nanocluster and paclitaxel-loaded charge-switchable nanohybrids for MR imaging and chemotherapy. *J Mater Chem B*. 2017;5(4):849–857.
52. Yuan YY, Mao CQ, du XJ, du JZ, Wang F, Wang J. Surface charge switchable nanoparticles based on zwitterionic polymer for enhanced drug delivery to tumor. *Adv Mater*. 2012;24(40):5476–5480.
53. Wu H, Cabral H, Toh K, et al. Polymeric micelles loaded with platinum anticancer drugs target preangiogenic micrometastatic niches associated with inflammation. *J Control Release*. 2014;189:1–10.
54. Bao Y, Guo Y, Zhuang X, et al. D-α-tocopherol polyethylene glycol succinate-based redox-sensitive paclitaxel prodrug for overcoming multidrug resistance in cancer cells. *Mol Pharm*. 2014;11(9):3196–3209.
55. Hou L, Yao J, Zhou J, Zhang Q. Pharmacokinetics of a paclitaxel-loaded low molecular weight heparin-all-trans-retinoid acid conjugate ternary nanoparticulate drug delivery system. *Biomaterials*. 2012;33(21):5431–5440.

Supplementary materials

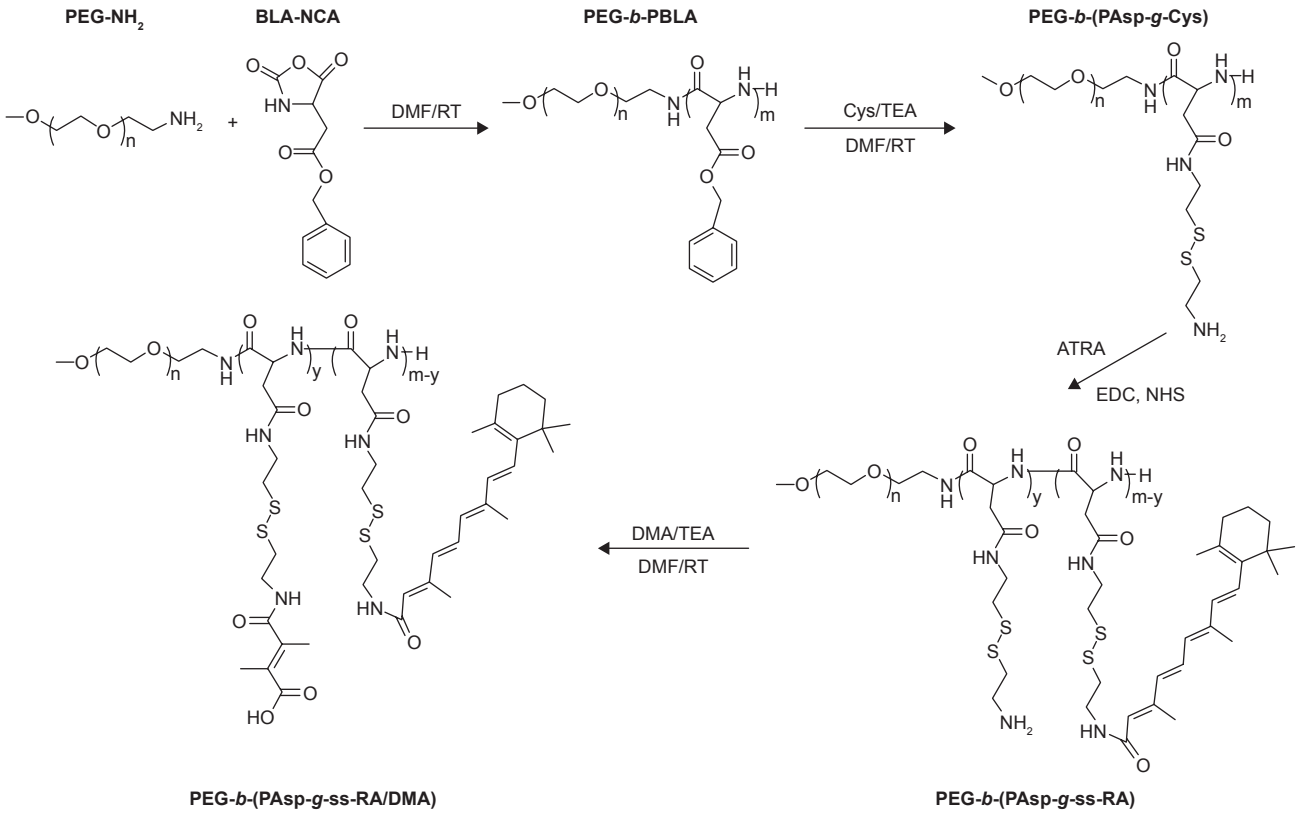

Scheme S1 The synthesis route of PEG-*b*-(PAsp-*g*-ss-RA/DMA).

Abbreviations: PEG, polyethylene glycol; BLA-NCA, β-benzyl-L-aspartate-*N*-carboxy-anhydride; PBLA, poly(β-benzyl-L-aspartate-*N*-carboxy-anhydride); Cys, cystamine dihydrochloride; ATRA, all-*trans*-retinoic acid; DMA, 2,3-dimethylmalefic anhydride; DMF, N,N-dimethylformamide; RT, room temperature; TEA, triethylamine; EDC, 3 (ethyliminomethylideneamino)-N,N-dimethylpropan-1-amine,hydrochloride; NHS, n-hydroxysuccinimide; RA, all-*trans*-retinoic acid; ^{1}H NMR, nuclear magnetic resonance.

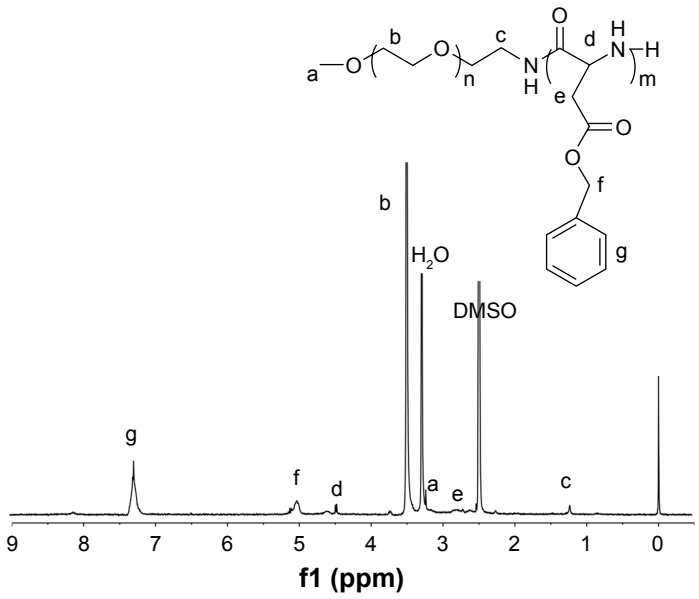

Figure S1 ^{1}H NMR spectra of PEG-*b*-PBLA in DMSO-d6.

Abbreviations: PEG, polyethylene glycol; PBLA, poly(β-benzyl-L-aspartate-*N*-carboxy-anhydride); DMSO, dimethyl sulfoxide; ^{1}H NMR, nuclear magnetic resonance.

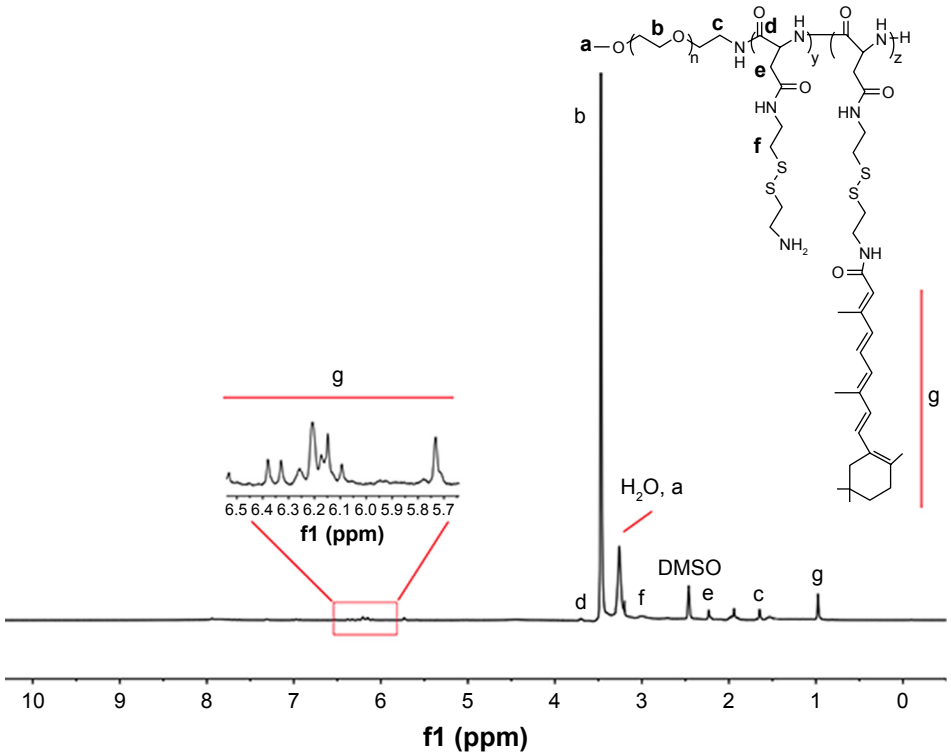

Figure S2 ^{1}H NMR spectra of PEG-*b*-(PAsp-*g*-ss-AR).
Abbreviations: PEG, polyethylene glycol; DMSO, dimethyl sulfoxide; ^{1}H NMR, nuclear magnetic resonance; RA, all-*trans*-retinoic-acid.

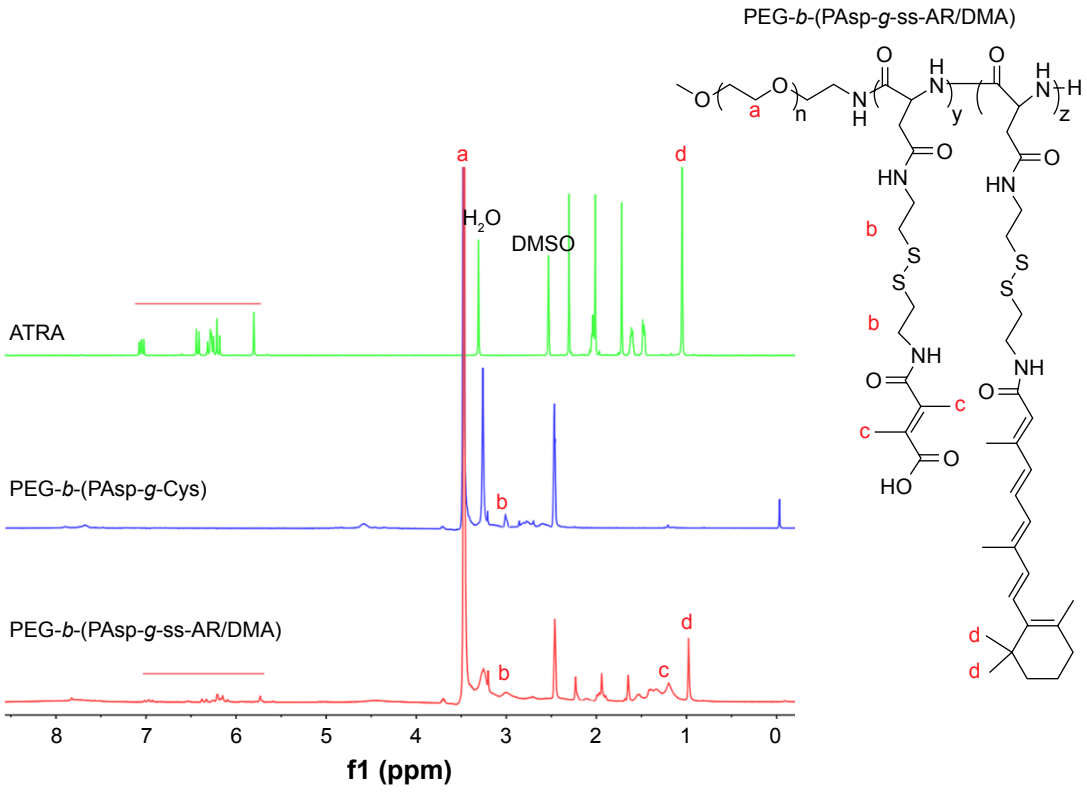

Figure S3 ^{1}H NMR spectra of ATRA, PEG-*b*-(PAsp-*g*-Cys) and PEG-*b*-(PAsp-*g*-ss-AR/DMA) in DMSO-*d6*.
Abbreviations: ATRA, all-*trans*-retinoic acid; PEG, polyethylene glycol; Cys, cystamine dihydrochloride; DMA, 2,3-dimethylmalefic anhydride; DMSO, dimethyl sulfoxide; RA, all-*trans*-retinoic-acid.

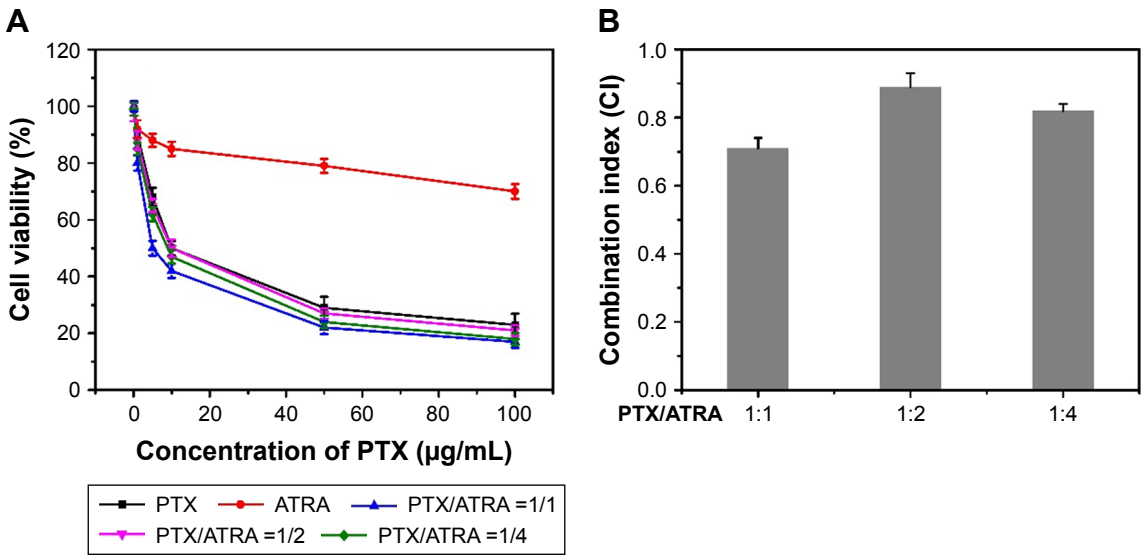

Figure S4 (**A**) Viability of A549 cells incubated with free PTX, free ATRA and PTX+ATRA with a different mass ratio for 48 hours at the different drug concentrations. (**B**) The CI of different drug ratio.
Abbreviations: PTX, paclitaxel; ATRA, all-*trans*-retinoic acid; CI, combination index.

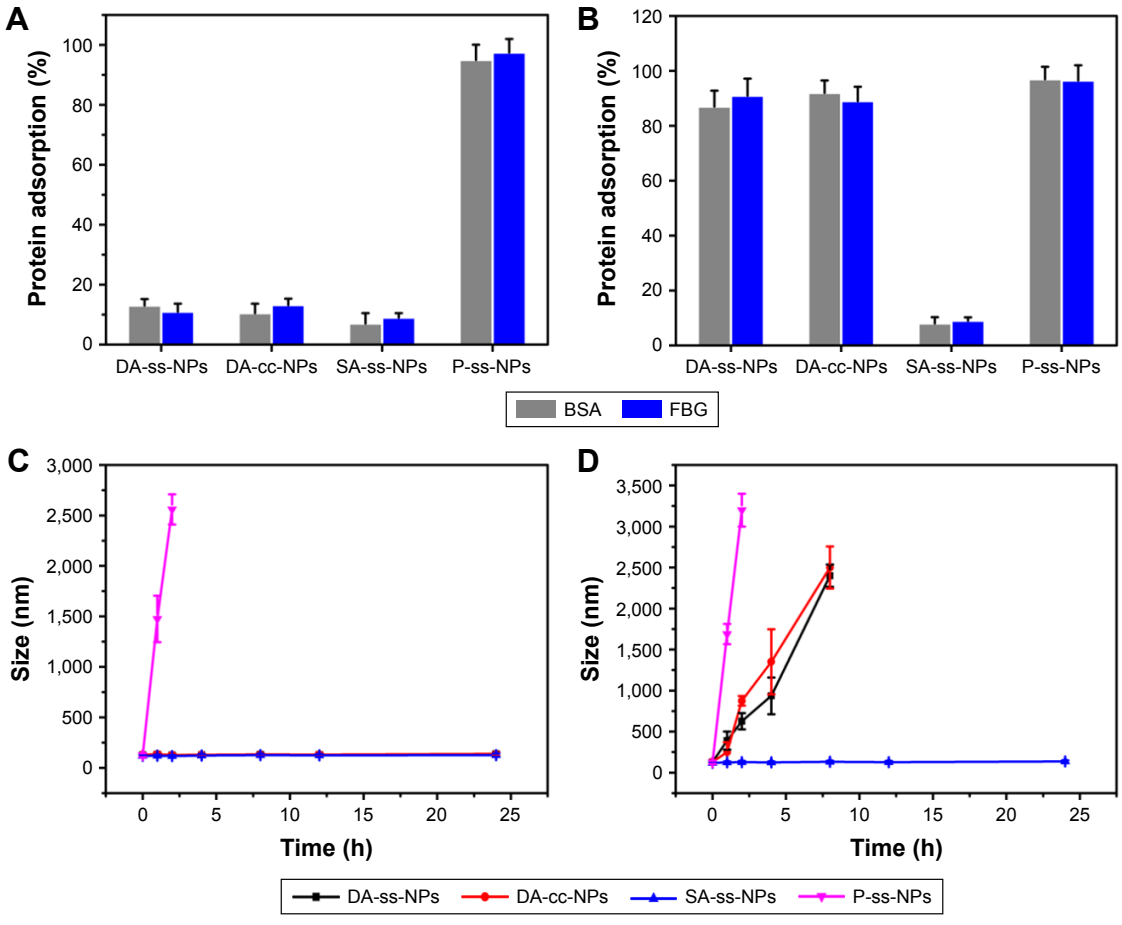

Figure S5 BSA and FBG adsorption of DA-ss-NPs, DA-cc-NPs, SA-ss-NPs and P-ss-NPs at pH 7.4 (**A**) or pH 6.5 (**B**), mean±SD, n=3. Changes in particle size of DA-ss-NPs, DA-cc-NPs, SA-ss-NPs and P-ss-NPs following incubation with RPMI 1640 culture medium with 10 FBS at pH 7.4 (**C**) or pH 6.5 (**D**); the diameters of all micelles at time 0 were determined in PBS, mean±SD, n=3.
Abbreviations: FBG, fibrinogen; RPMI, Roswell Park Memorial Institute.